P3A.9 **COMPARISONS OF RAINDROP SIZE DISTRIBUTIONS FROM THE TRMM PRECIPITATION RADAR AND THE C-POL GROUND RADAR**

Yuxiang Liu *, V. N. Bringi
Colorado State University, Fort Collins, Colorado
T. D. Keenan
BMRC, Melbourne, Vic., Australia

1. INTRODUCTION

Because of the high frequency (13.8GHz) used in the TRMM PR, attenuation correction plays a very important role in obtaining the correct estimated reflectivity (Z_e) and hence the rain rate. In version 5 of 2A25 data product, a global (rain type dependent) initial specific attenuation and reflectivity, $k=\alpha Z^{\beta}$, relation is assumed (Iguchi et al 2000). Combined with surface reference technique (srt), a multiplicative adjustment factor, ε_f, is estimated to adjust α in the initial relation. From the initial value of α, ε_f, and the weight factor w, the drop size distribution (dsd) parameters (N_w, D_0) can be retrieved (note that the shape parameter μ is fixed at 3 in this algorithm). The D_0 is retrieved using Z and N_w. At the same time, dsd parameters can also be retrieved from ground-based radar (Bringi et al 2001). It is useful to compare these two retrievals from two different instruments. In this study, the C-POL radar is used to retrieve the dsd parameters from polarimetric measurements, i.e., Z_h, Z_{dr}, K_{dp}, in 3 different locations, i.e., Darwin, South China Sea (SCSMEX), and Sydney, respectively. Scatterplots for N_w and D_0 in convective and stratiform rain are presented.

2. DROP SIZE DISTRIBUTION RETRIEVALS

It is well known that the srt can be used to narrow the possible range of the dsd parameters. Subsequently, an altered N_w value for the beam may be inferred (e.g. Ferreira et al 2001). Our analysis indicates that $N_w=19{,}365\varepsilon_0^{4.37}$ for convective rain, and $N_w=7018\varepsilon_0^{4.815}$ for stratiform rain at the lowest altitudes of interest, based on the version 5 2A25 initial k-Z relations in Iguchi et al (2000) and our own analysis of k/N_w versus Z/N_w based on Darwin dsds as measured by a disrometer (entire season of disdrometer measurements). Note that herein ε_0 from pure srt is used instead of ε_f from the combined method (Iguchi et al 2000). The ε_f and ε_0 are related by $\varepsilon_f=1-w+w\varepsilon_0$.

* *Corresponding author address:* Yuxiang Liu, Colorado State Univ., Dept. of Electrical Engineering, Ft. Collins, CO 80523; e-mail: liuyx@engr.colostate.edu.

Our analysis focuses on those PR beams with large PIA (e.g., >=5dB) and w>=0.01. If this is not achievable, the intial dsd is used to avoid abnormal values of ε_0. Subsequently, we estimate D_0 using a power law fit of the form $(Z/N_w)=cD_0^b$ where c and b are based on Darwin disdrometer data alluded to earlier. Once normalized variables are used the coefficient c does not depend on rain rate and the exponent b is only very weakly dependent on the shape parameter μ. This is one possible method to estimate N_w and D_0 from the PR data but is sufficient here for comparing with C-POL radar retrievals. We used the same k/N_w versus Z/N_w relation for other locations, since it is relatively insensitive to dsd changes.

The C-band version of the dsd retrieval algorithm is described in Bringi et al (2002).

3. PROCESSING OF THE PR AND GR DATA

The different resolution sizes and different viewing aspects between the PR and the GR should be taken into account before analysis can take place. It is also helpful to correct for the geometry distortion due to space radar movement (Bolen and Chandrasekar 2002). An alignment program is run to create overlapping images from PR and GR raw data, e.g. 1B21, 1C21, 2A23 and 2A25 from PR, and UF files from GR. For comparison, the time delay between the two data sets is chosen not to exceed 10 minutes. After processing, two 50 by 50 km 2-D and 3-D data sets are generated for PR and GR, resulting in grid points with the same resolution. In particular, GR horizontal resolution is downgraded to 4 by 4 km, while both GR and PR vertical resolutions are downgraded to 0.5 km.

As stated earlier, storm events from Darwin, SCSMEX and Sydney were analyzed. There are a total of 8 events, including 5 over-ocean events and 3 over-land events. Table 1 shows the location site, date, time, and land/ocean flag for each event.

4. DSD COMPARISONS

Figure 1 shows N_w vs. D_0 scatterplot comparisons in convective rain and in stratiform rain at different sites. Note that these N_w and D_0 values were taken from layers between 2 and 3km, where we could avoid melting ice particles in these events, and have sufficient sample grid points to conduct a statistical analysis.

TABLE 1

#	Location	Date (yy/mm/dd)	Time (UTC)	Land/ Ocean
1	Darwin	99/12/27	03:00:09-03:07:46	Land
2	Darwin	00/02/03	07:20:08-07:27:43	Ocean
3	SCSMEX	98/05/16	01:30:12-01:38:18	Ocean
4	SCSMEX	98/05/19	07:30:11-07:38:23	Ocean
5	Sydney	00/09/26	00:10:31-00:18:58	Ocean
6	Sydney	00/09/26	21:30:10-21:38:38	Ocean
7	Sydney	00/11/03	04:20:09-04:28:31	Land
8	Sydney	00/12/18	05:00:10-05:08:45	Land

Figure 2 shows the median $\log_{10}N_w$ vs. D_0 for convective rain in each event.

For convective rain, we observed different dsd comparisons over land and over ocean. As the scatterplots show, the ranges of scatter for PR and for GR for convective rain over ocean are similar. However, for convective rain over land, the ranges from the two radars are different, most evident in events in Sydney. We observed a tendency for lower N_w values and higher D_0 values retrieved by the PR in these over land events (relative to the GR retrievals). At the same time, figure 2 shows the similar observations by median values, as we can see there is the same tendency in land events but not in ocean events.

For stratiform rain, we could not get sufficient sample points to show a scatter for PR. Typically, in stratiform rain where the PIA was low, the weighting towards srt method will be very low considering the reliability of the difference in radar cross section between rain-free and raining area. Therefore, the initial dsd would be in place. Although we could not get the PR dsd values to scatter, we were able to see that the initial values were placed in the center of the GR scatter, indicating that the initial values for stratiform rain may be reliable.

5. CONCLUSION

DSD comparisons between PR retrievals and GR retrievals were presented. General good agreement was observed in over-ocean storm events. This indicates the 2A25 profiling algorithm is generally unbiased according to the GR observations. However, in over-land storm events, N_w and D_0 bias were observed. In particular, when GR retrievals were used as reference, the PR-N_w values tended to be systematically on the lower side and PR-D_0 tended to be systematically on the higher side. This indicates a possible bias in the PR retrieval of N_w and D_o for strong convective rain over land which may be related to the different statistics of ε_0 over land (as opposed to ocean).

6. ACKNOWLEDGEMENTS

This research was supported by the NASA TRMM grant NAG5-7717.

7. REFERENCES

Bolen, S. and V. Chandrasekar, 2002: Methodology for aligning and comparing spaceborne radar and ground-based radar observations. *J. Atmos. Ocean. Tech.*, **20**, 647-659.

Bringi, V.N., and V. Chandrasekar, 2001: Polarimetric doppler weather radar: principles and applications. *Cambridge Univ. Press*, pp. 636.

Ferreira, F., P. Amayenc, S. Oury, and J. Testud, 2001: Study and tests of improved rain estimates from the TRMM Precipitation Radar. *J. Appl. Meteo.*, **40**, 1878-1899.

Iguchi, T., T. Kozu, R. Meneghini, J. Awaka, and K. Okamoto, 2000: Rain-profiling algorithm for the TRMM Precipatation Radar. *J. Appl. Meteo.*, **39**, 2038-2052

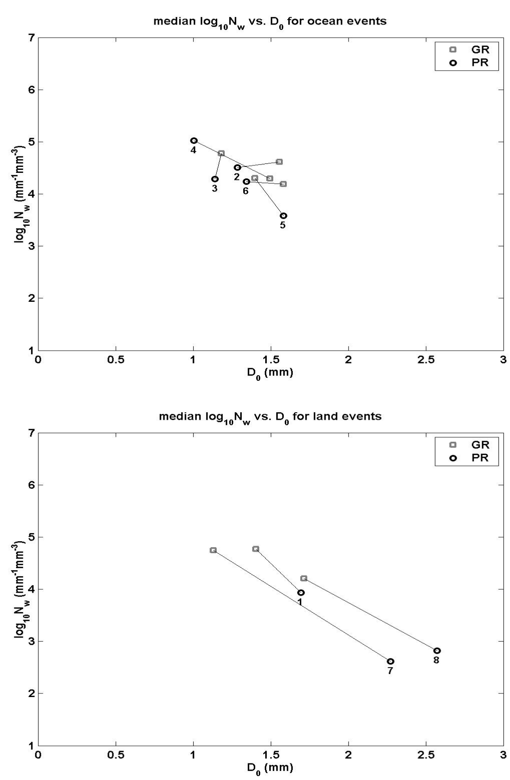

Figure 2

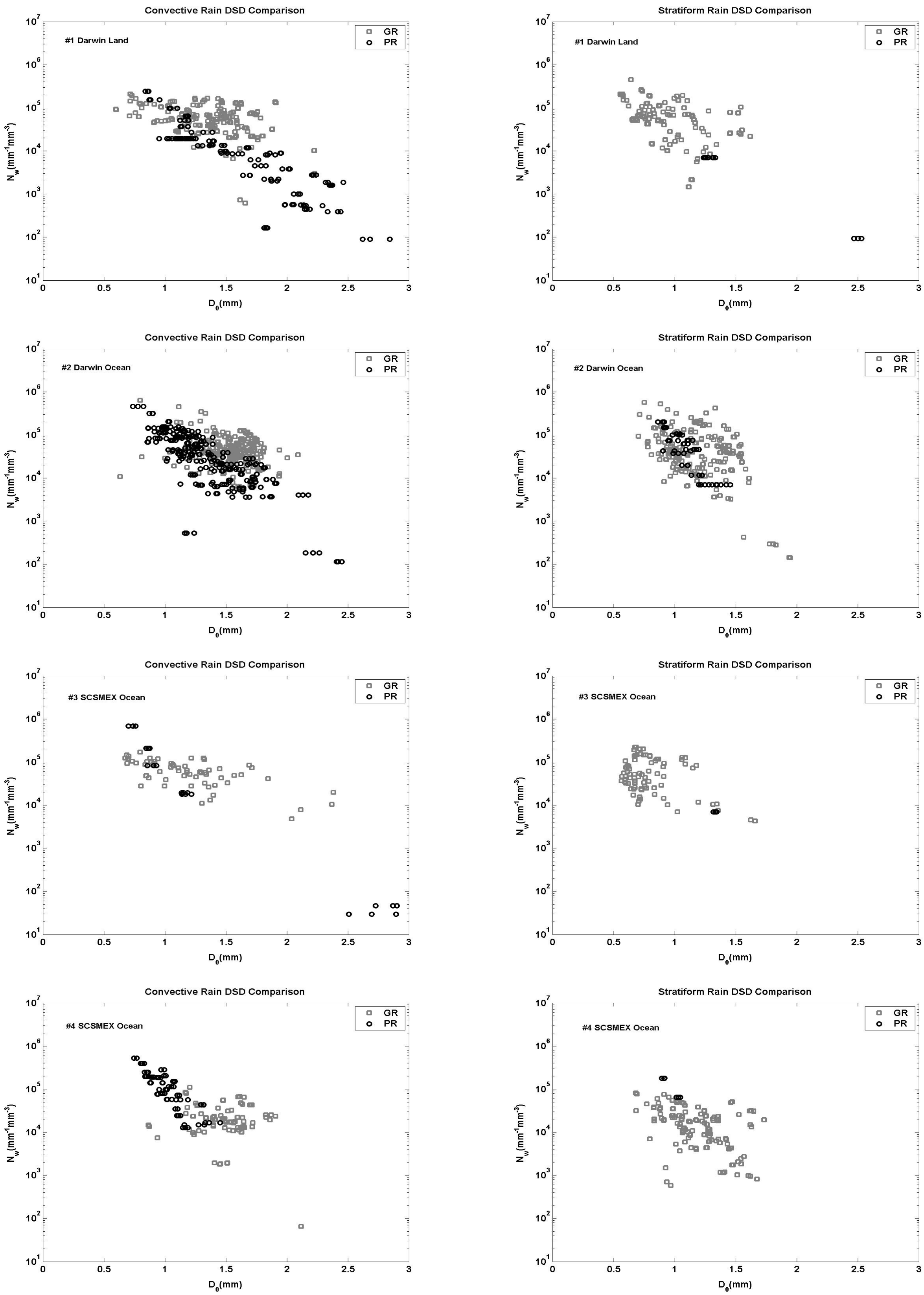

Convective Rain DSD Comparison
#1 Darwin Land
GR
PR
Stratiform Rain DSD Comparison
#1 Darwin Land
GR
PR
Convective Rain DSD Comparison
#2 Darwin Ocean
GR
PR
Stratiform Rain DSD Comparison
#2 Darwin Ocean
GR
PR
Convective Rain DSD Comparison
#3 SCSMEX Ocean
GR
PR
Stratiform Rain DSD Comparison
#3 SCSMEX Ocean
GR
PR
Convective Rain DSD Comparison
#4 SCSMEX Ocean
GR
PR
Stratiform Rain DSD Comparison
#4 SCSMEX Ocean
GR
PR
$N_w(mm^{-1}mm^{-3})$
$D_0(mm)$

Figure 1

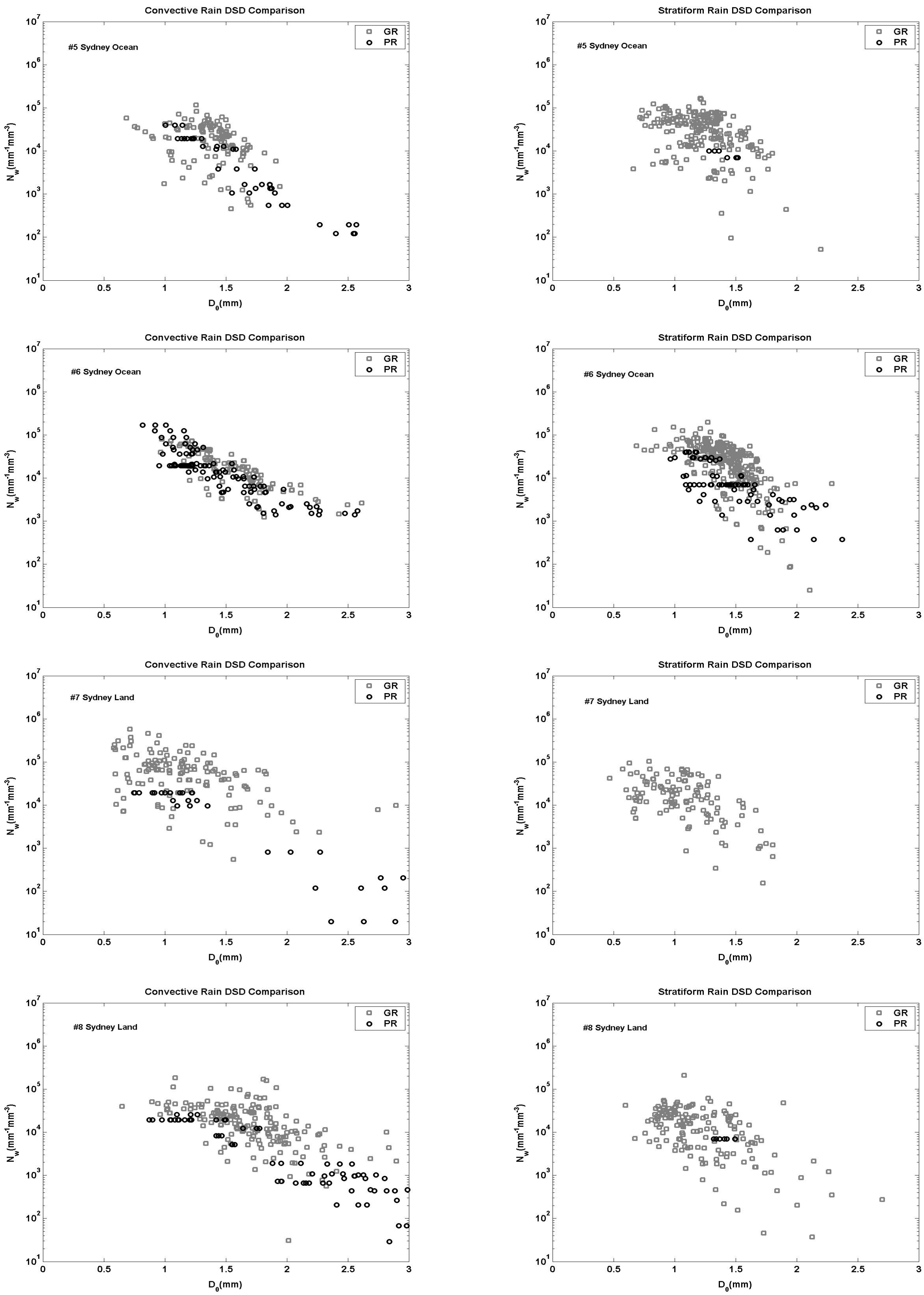

Figure 1 (continued)